Role of ANKHD1/LINC00346/ZNF655 Feedback Loop in Regulating the Glioma Angiogenesis via Staufen1-Mediated mRNA Decay

Chunqing Yang,[1,2,3] Jian Zheng,[1,2,3] Xiaobai Liu,[1,2,3] Yixue Xue,[4,5,6] Qianru He,[4,5,6] Yiming Dong,[1,2,3] Di Wang,[1,2,3] Zhen Li,[1,2,3] Libo Liu,[4,5,6] Jun Ma,[4,5,6] Heng Cai,[1,2,3] and Yunhui Liu[1,2,3]

[1]Department of Neurosurgery, Shengjing Hospital of China Medical University, Shenyang 110004, China; [2]Liaoning Clinical Medical Research Center in Nervous System Disease, Shenyang 110004, China; [3]Key Laboratory of Neuro-oncology in Liaoning Province, Shenyang 110004, China; [4]Department of Neurobiology, College of Basic Medicine, China Medical University, Shenyang 110122, China; [5]Key Laboratory of Cell Biology, Ministry of Public Health of China, China Medical University, Shenyang 110122, China; [6]Key Laboratory of Medical Cell Biology, Ministry of Education of China, China Medical University, Shenyang 110122, China

Accumulating evidence shows that long noncoding RNA (lncRNA) dysregulation plays a critical role in tumor angiogenesis. Glioma is characterized by abundant angiogenesis. Herein, we investigated the expression and function of LINC00346 in the regulation of glioma angiogenesis. The present study first demonstrated that ANKHD1 (ankyrin repeat and KH domain-containing protein 1) and LINC00346 were significantly increased in glioma-associated endothelial cells (GECs), whereas ZNF655 (zinc finger protein 655) was decreased in GECs. Meanwhile, ANKHD1 inhibition, LINC00346 inhibition, or ZNF655 overexpression impeded angiogenesis of GECs. Moreover, ANKHD1 targeted LINC00346 and enhanced the stability of LINC00346. In addition, LINC00346 bound to ZNF655 mRNA through their Alu elements so that LINC00346 facilitated the degradation of ZNF655 mRNA via a STAU1 (Staufen1)-mediated mRNA decay (SMD) mechanism. Futhermore, ZNF655 targeted the promoter region of ANKHD1 and formed an ANKHD1/LINC00346/ZNF655 feedback loop that regulated glioma angiogenesis. Finally, knockdown of ANKHD1 and LINC00346, combined with overexpression of ZNF655, resulted in a significant decrease in new vessels and hemoglobin content *in vivo*. The results identified an ANKHD1/LINC00346/ZNF655 feedback loop in the regulation of glioma angiogenesis that may provide new targets and strategies for targeted therapy against glioma.

INTRODUCTION

Glioma is the most common tumor of the human central nervous system, which is characterized by its high degree of malignancy, high invasiveness, and poor prognosis. The median survival time of patients with glioma is still only 12 to 18 months, despite improvements in surgery, radiotherapy, and chemotherapy.[1] Numerous studies have shown that the formation of new blood vessels is involved in the process of tumor growth and metabolism. Thus, angiogenesis is considered to be a marker of the development and progression of malignant tumors.[2] Glioma is a solid tumor of which the growth and metastasis are dependent on angiogenesis.[3]

Therefore, anti-angiogenesis therapy has become an effective method for the treatment of glioma.

RNA binding proteins (RBPs) play critical roles in every step of gene expression, especially in the regulation of transcription and post-transcriptional processes.[4] RBPs mediate mRNA splicing, the maintenance of RNA stability, and translation through the identification of specific mRNA components.[5] Recent data suggest that RBPs are involved in regulating the development and progression of multiple tumors. For example, NOVA1 acts as an oncogene in melanoma development.[6] Overexpression of QKI-5 significantly decreases proliferation and transformation of lung cancer cells.[7] The ankyrin repeat and KH domain-containing protein 1 (ANKHD1) is an RBP and plays a role in the regulation of the cell cycle and transcription.[8] ANKHD1 is upregulated in several tumor cells (e.g., multiple myeloma and acute leukemia) and significantly reduces patient survival.[9,10] However, the expression of ANKHD1 in glioma-associated endothelial cells (GECs) compared with astrocyte-associated endothelial cells (AECs) and the function of ANKHD1 in the regulation of angiogenesis remain poorly defined.

Long noncoding RNAs (lncRNAs) belong to the noncoding genes that consist of more than 200 nucleotides. Accumulating evidence shows that lncRNAs are singularly expressed in many malignancies and may be related to the modulation of tumor development.[11] For instance, Linc00176 is upregulated during the malignant progression of hepatocellular carcinoma cells.[12] Brain-derived neurotrophic factor-antisense (BDNF-AS) is downregulated in prostate cancer tissues and cells and predictive of poor prognosis.[13] The abnormal expression lncRNA-LINC00346 was filtered out using lncRNA microarray analysis in our study. LINC00346 is highly expressed in bladder
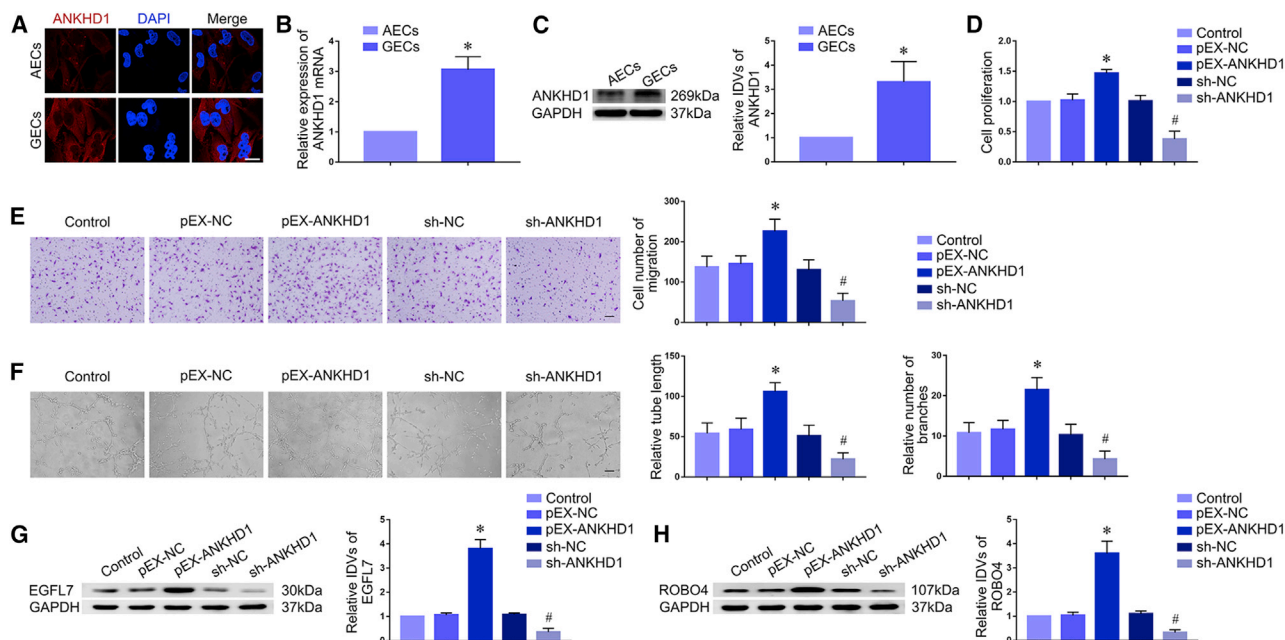
Figure 1. ANKHD1 Expression in GECs and Silencing of ANKHD1 Inhibited the Angiogenesis of GECs

(A) Immunofluorescence staining was used to detect the expression and location of ANKHD1 in GECs and AECs (red, ANKHD1; blue, 4′,6-diamidino-2-phenylindole [DAPI] nuclear staining). Scale bar, 20 μm. (B) Quantitative real-time PCR was conducted to measure the relative expression levels of ANKHD1 mRNA in AECs and GECs using glyceraldehyde 3-phosphate dehydrogenase (GAPDH) as an endogenous control. Data are presented as the mean ± SD (n = 3, each group). *p < 0.05 versus AEC group. (C) Western blot was used to detect ANKHD1 protein expression levels in AECs and GECs using GAPDH as an endogenous control. Data are presented as the mean ± SD (n = 3, each group). *p < 0.05 versus AEC group. (D) CCK-8 assay was conducted to evaluate the proliferation effect of overexpression or knockdown of ANKHD1 on GECs. (E) Transwell assay was used to measure the quantification number of migration cells with overexpression or knockdown of ANKHD1. (F) Matrigel tube formation assay was applied to determine the effect of overexpression or knockdown of ANKHD1 on the tube formation of GECs. Representative images and corresponding statistical plots are presented. Data are presented as the mean ± SD (n = 3, each group). *p < 0.05 versus pEX-NC group; #p < 0.05 versus sh-NC group. Scale bars, 30 μm. (G and H) Western blot analysis for ANKHD1-regulated EGFL7 (G) and ROBO4 (H) expression in GECs. The relative IDVs of EGFL7 and ROBO4 were shown using GAPDH as an endogenous control. Data are presented as the mean ± SD (n = 3, each group). *p < 0.05 versus pEX-NC group; #p < 0.05 versus sh-NC group.

cancer and functions as an oncogene.[14] However, the expression and function of LINC00346 in GECs remain unclear.

The Staufen1 (STAU1)-mediated mRNA decay (SMD) is involved in the regulation of functional mRNAs and transcription.[15] STAU1 is a double-stranded RNA-binding protein that binds to the STAU1-binding site (SBS) in the 3′ untranslated region (3′ UTR) of target mRNA.[16,17] UPF1 is an evolutionarily conserved and ubiquitously expressed phosphoprotein. STAU1 recruits UPF1 to mediate rapid mRNA degradation by SMD.[18]

Zinc finger protein 655 (ZNF655) belongs to the Krüppel-like zinc-finger gene family. ZNF655 regulates the cell-cycle progression of HeLa cells.[19] In this study, mRNA microarray data indicated the differentially expressed ZNF655 in GECs treated with short hairpin (sh)-LINC00346. However, its function in glioma angiogenesis requires further investigation.

Epidermal growth factor-like domain 7 (EGFL7) and Roundabout4 (ROBO4) are both angiogenic factors that are highly expressed in many malignant tumor tissues and cells (e.g., cervical, pancreatic,

and breast cancer[20–22]). EGFL7 and ROBO4 both have been recognized as the biomarkers of tumor angiogenesis. Recent studies have shown that EGFL7 and ROBO4 are both highly expressed in glioma tissues and cells and promote glioma angiogenesis.[23,24]

In the present study, we investigated the expression of ANKHD1, LINC00346, and ZNF655; their interactions in GECs; and their roles in the regulation of glioma angiogenesis. The results of this study may provide new targets for anti-angiogenesis therapy against glioma and new ideas for targeted therapy.

RESULTS

ANKHD1 Is Upregulated in GECs, and Knockdown of ANKHD1 Inhibits the Angiogenesis of GECs

Immunofluorescence staining, quantitative real-time PCR and western blot were used to detect the endogenous expression of ANKHD1. ANKHD1 was mainly located in the cytoplasm and was significantly increased in the GEC group (Figure 1A). The mRNA and protein expression levels of ANKHD1 were significantly upregulated in the GEC group (Figures 1B and 1C). A cell counting kit-8 (CCK-8) assay was conducted to determine that overexpression of ANKHD1
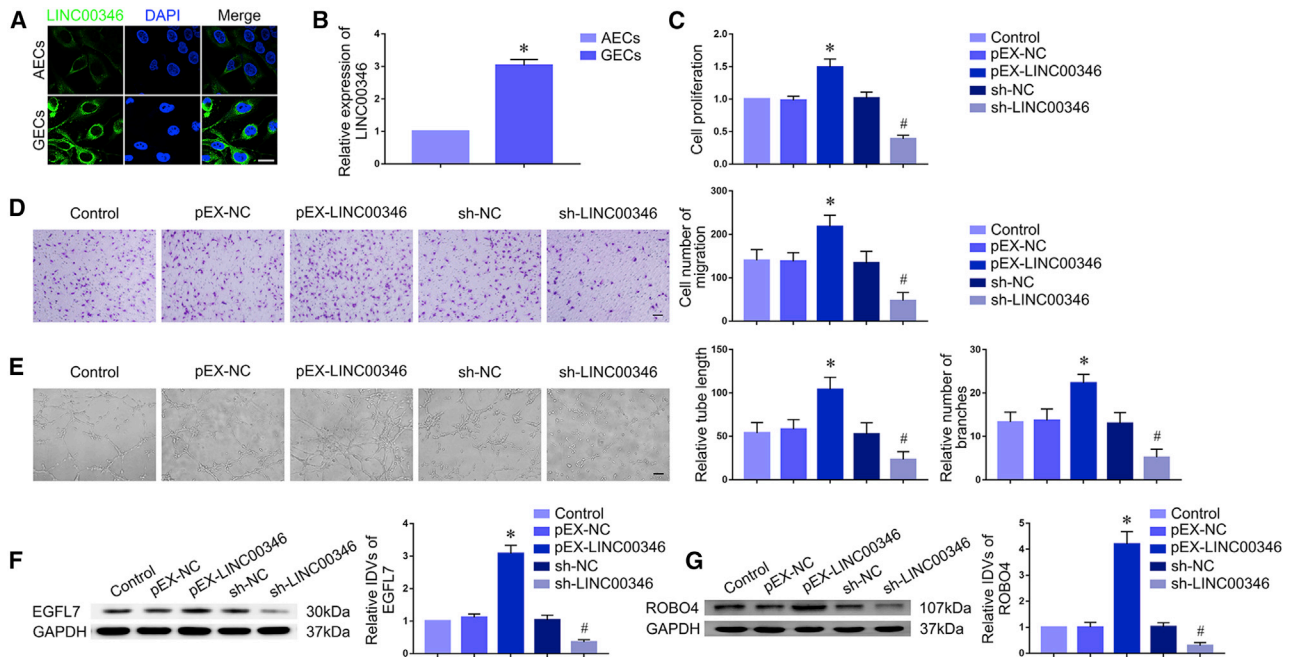
Figure 2. LINC00346 Expression in GECs and Downregulation of LINC00346 Suppressed the Angiogenesis of GECs

(A) FISH was used to detect the expression and location of LINC00346 in GECs and AECs (green, LINC00346; blue, DAPI nuclear staining). Scale bar, 20 μm. (B) Quantitative real-time PCR was conducted to measure the relative expression levels of LINC00346 in AECs and GECs using GAPDH as an endogenous control. Data are presented as the mean ± SD (n = 3, each group). *p < 0.05 versus AEC group. (C) CCK-8 assay was conducted to evaluate the proliferation effect of overexpression or knockdown of LINC00346 on GECs. (D) Transwell assay was used to measure the quantification number of migration cells with overexpression or knockdown of LINC00346. (E) Matrigel tube formation assay was applied to determine the effect of overexpression or knockdown of LINC00346 on the tube formation of GECs. Representative images and corresponding statistical plots are presented. Data are presented as the mean ± SD (n = 3, each group). *p < 0.05 versus pEX-NC group; #p < 0.05 versus sh-NC group. Scale bars, 30 μm. (F and G) Western blot analysis for LINC00346-regulated EGFL7 (F) and ROBO4 (G) expression in GECs. The relative IDVs of EGFL7 and ROBO4 were shown using GAPDH as an endogenous control. Data are presented as the mean ± SD (n = 3, each group). *p < 0.05 versus pEX-NC group; #p < 0.05 versus sh-NC group.

significantly increased the viability of GECs, whereas inhibition of ANKHD1 exhibited the opposite results (Figure 1D). A Transwell assay was used to evaluate that overexpression of ANKHD1 significantly increased migrating cell numbers of GECs, whereas inhibition of ANKHD1 exhibited the opposite results (Figure 1E). A Matrigel tube formation assay was conducted to verify that overexpression of ANKHD1 significantly increased relative tube length and number of branches of GECs, whereas inhibition of ANKHD1 exhibited the opposite results (Figure 1F). Further, EGFL7 and ROBO4 protein expression were significantly increased in the pEX-ANKHD1 group, whereas inhibition of ANKHD1 led to a marked decrease (Figures 1G and 1H).

LINC00346 Is Upregulated in GECs, and Knockdown of LINC00346 Inhibits the Angiogenesis of GECs

With the use of lncRNA microarray analysis and quantitative real-time PCR, we demonstrated that LINC00346 was significantly decreased in GECs treated with sh-ANKHD1 (Figures S1A and S1B) so that we selected LINC00346 for research, for which the change in expression was the most obvious. Fluorescence in situ hybridization (FISH) was used to demonstrate that LINC00346 was mainly located in the cytoplasm and was markedly upregulated in the GEC group (Figure 2A). Further, quantitative real-time PCR

was used to detect that LINC00346 was remarkably highly expressed in the GEC group (Figure 2B). In addition, overexpression of LINC00346 significantly promoted the proliferation, migration, and tube formation of GECs, whereas inhibition of LINC00346 showed a prominent inhibitory effect (Figures 2C–2E). In addition, EGFL7 and ROBO4 protein expression was significantly increased in the pEX-LINC00346 group, whereas the protein expression was significantly decreased in the sh-LINC00346 group (Figures 2F and 2G).

ANKHD1 Targets LINC00346 and Regulates the Angiogenesis of GECs via Stabilizing LINC00346

With the use of bioinformatics databases (RBPmap), we predicted that ANKHD1 might bind to LINC00346. RNA immunoprecipitation (RIP) results showed that the enrichment of LINC00346 was higher in the anti-ANKHD1 group than that in the anti-immunoglobulin G (IgG) group (Figure 3A). Meanwhile, we examined the expression of LINC00346 in GECs transfected with ANKHD1. LINC00346 expression was significantly decreased in the sh-ANKHD1 group (Figure 3B). Besides, the results indicated that there was no significant difference of the relative expression of nascent LINC00346 in pEX-ANKHD1 (Figure 3C). Furthermore, we detected that the half-life of LINC00346 was significantly shortened in sh-ANKHD1, for which GECs were
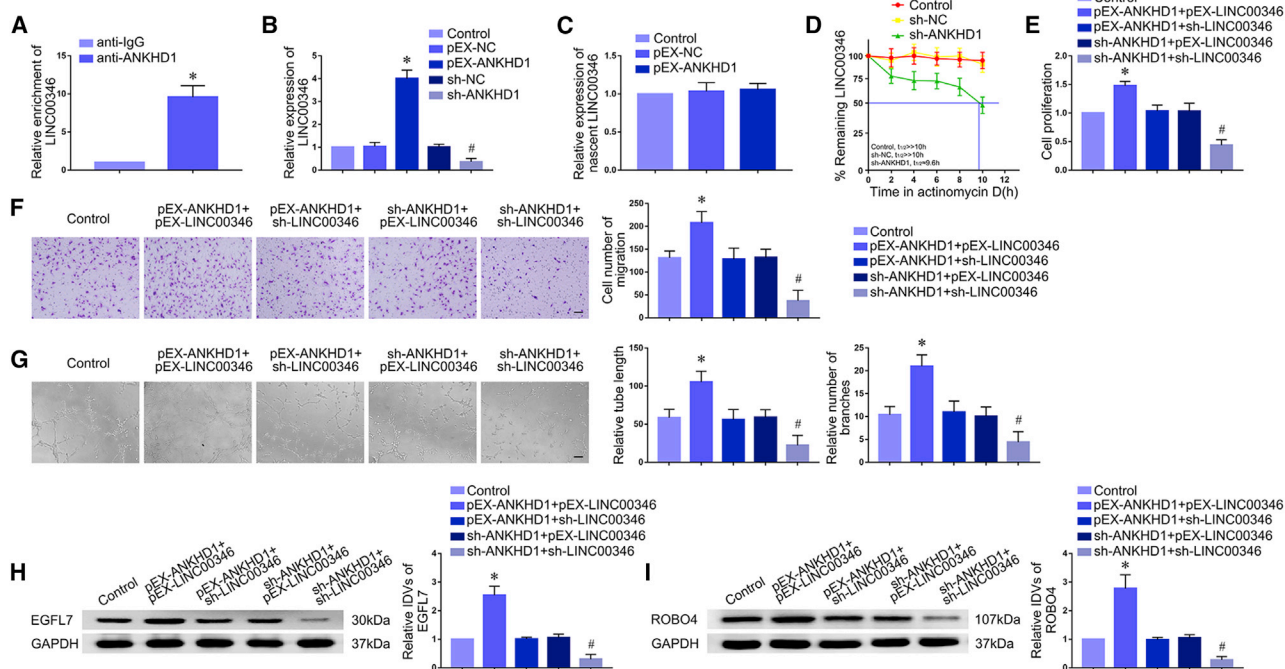
Figure 3. ANKHD1 Regulated the Angiogenesis of GECs by Targeting and Stabilizing LINC00346

(A) LINC00346 was identified in the ANKHD1 complex by the RIP assay. Relative enrichment of LINC00346 was measured using quantitative real-time PCR. Data are presented as the mean ± SD (n = 3, each group). *p < 0.05 versus anti-IgG group. (B) Quantitative real-time PCR for ANKHD1-regulated LINC00346 expression in GECs. The relative expression of LINC00346 was shown using GAPDH as an endogenous control. Data are presented as the mean ± SD (n = 3, each group). *p < 0.05 versus pEX-NC group; #p < 0.05 versus sh-NC group. (C) Quantitative real-time PCR was conducted to measure the expression of nascent LINC00346 in the control group, pEX-NC group, and pEX-ANKHD1 group. (D) The graph represented the relative levels of the LINC00346 at the different actinomycin D treatment times in the control group, sh-NC group, and sh-ANKHD1 group. (E) CCK-8 assay was conducted to evaluate the proliferation effect of ANKHD1 and LINC00346 on GECs. (F) Transwell assay was used to measure the quantification number of migration cells with the expression of ANKHD1 and LINC00346. (G) Matrigel tube formation assay was applied to determine the effect of ANKHD1 and LINC00346 on the tube formation of GECs. Representative images and corresponding statistical plots are presented. Data are presented as the mean ± SD (n = 3, each group). *p < 0.05 versus control group; #p < 0.05 versus control group. Scale bars, 30 μm. (H and I) Western blot analysis for ANKHD1 combined with LINC00346-regulated EGFL7 (H) and ROBO4 (I) expression in GECs. The relative IDVs of EGFL7 and ROBO4 were shown using GAPDH as an endogenous control. Data are presented as the mean ± SD (n = 3, each group). *p < 0.05 versus control group; #p < 0.05 versus control group.

treated with actinomycin D (Figure 3D). Moreover, simultaneous over-expression of ANKHD1 and LINC00346 significantly increased the proliferation, migration, and tube formation of GECs, and simultaneous inhibition of ANKHD1 and LINC00346 showed a prominent inhibitory effect, whereas there were no significant changes in glioma angiogenesis in the pEX-ANKHD1 + sh-LINC00346 group and sh-ANKHD1 + pEX-LINC00346 group (Figures 3E–3G). Further, simultaneous over-expression of ANKHD1 and LINC00346 significantly increased EGFL7 and ROBO4 protein expression, and simultaneous inhibition of ANKHD1 and LINC00346 significantly decreased the protein expression, whereas there were no significant changes in the protein expression in the pEX-ANKHD1 + sh-LINC00346 group and sh-ANKHD1 + pEX-LINC00346 group (Figures 3H and 3I).

ZNF655 Is Downregulated in GECs, and Overexpression of ZNF655 Inhibits the Angiogenesis of GECs

With the use of mRNA microarray analysis and quantitative real-time PCR, we verified that ZNF655 was significantly increased in GECs treated with sh-linc00346 (Figures S1C and S1D), so that we selected

ZNF655 for research. ZNF655 was found to be located in both nucleus and cytoplasm in the cells and was decreased in GECs (Figure 4A). Also, ZNF655 mRNA and protein expression both exhibited low expression levels in GECs (Figures 4B and 4C). Further, overexpression of ZNF655 significantly inhibited the proliferation, migration, and tube formation of GECs, whereas inhibition of ZNF655 showed the opposite results (Figures 4D–4F). Moreover, EGFL7 and ROBO4 protein expression was significantly decreased in the ZNF655^{+} group, whereas the protein expression was significantly increased in the ZNF655^{−} group (Figures 4G and 4H).

LINC00346 Binds to STAU1 and Involves SMD to Promote the Degradation of ZNF655 mRNA by Targeting ZNF655 mRNA and Forming the SBS

With the use of IntaRNA software, we analyzed that ZNF655 mRNA-targeted LINC00346 in a sequence-specific manner in the 3′ UTR. Dual-luciferase gene reporter assays were conducted to demonstrate the interaction between LINC00346 and ZNF655 mRNA. Two putative binding sites were identified in ZNF655 mRNA. The luciferase activity in
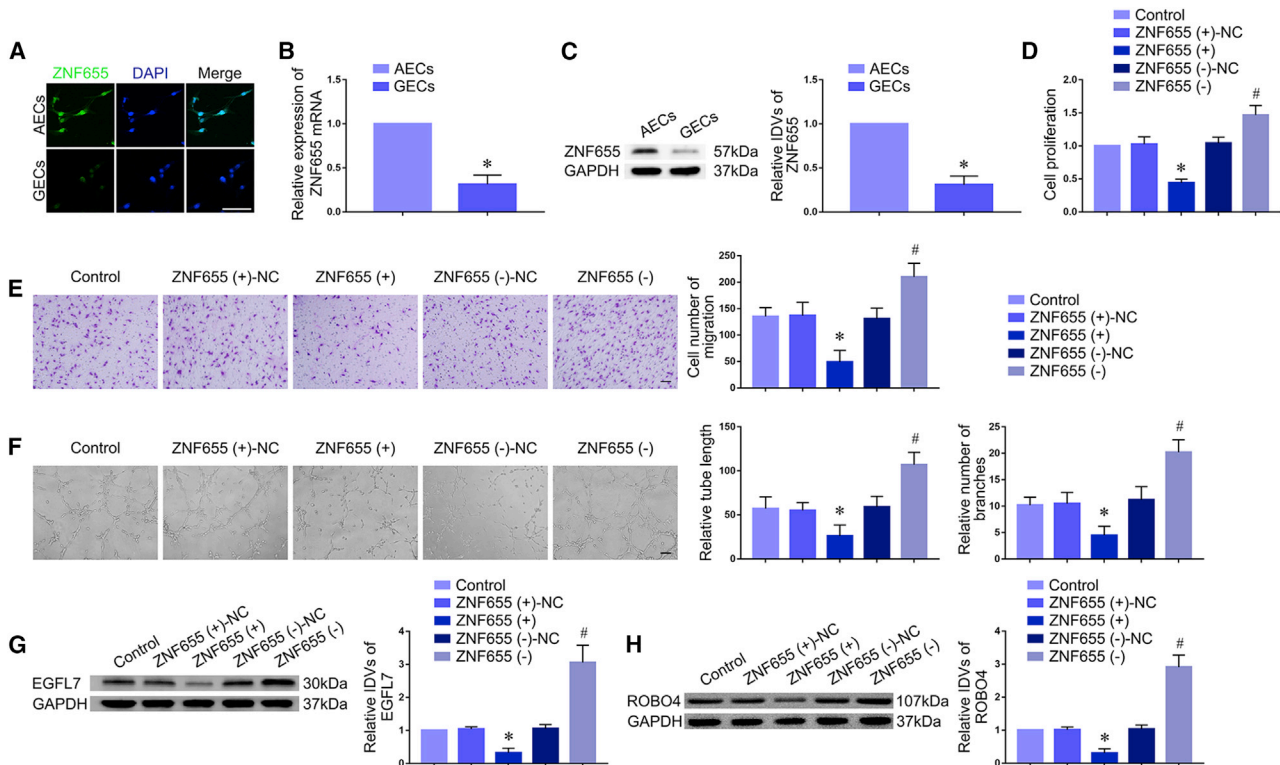
Figure 4. ZNF655 Was Lowly Expressed in GECs, and Overexpression of ZNF655 Restrained the Angiogenesis of GECs

(A) Immunofluorescence staining was used to detect the expression and location of ZNF655 in GECs and AECs (green, ZNF655; blue, DAPI nuclear staining). Scale bar, 20 μm. (B) Quantitative real-time PCR was conducted to measure the relative expression levels of ZNF655 mRNA in AECs and GECs. Data are presented as the mean ± SD (n = 3, each group). *p < 0.05 versus AEC group. (C) Western blot was used to detect ZNF655 protein expression levels in AECs and GECs. Data are presented as the mean ± SD (n = 3, each group). *p < 0.05 versus AEC group. (D) CCK-8 assay was conducted to evaluate the proliferation effect of overexpression or knockdown of ZNF655 on GECs. (E) Transwell assay was used to measure the quantification number of migration cells with overexpression or knockdown of ZNF655. (F) Matrigel tube formation assay was applied to determine the effect of overexpression or knockdown of ZNF655 on the tube formation of GECs. Representative images and corresponding statistical plots are presented. Data are presented as the mean ± SD (n = 3, each group). *p < 0.05 versus ZNF655 (+)-NC group; #p < 0.05 versus ZNF655⁻-NC group. Scale bars, 30 μm. (G and H) Western blot analysis for ZNF655-regulated EGFL7 (G) and ROBO4 (H) expression in GECs. The relative IDVs of EGFL7 and ROBO4 were shown using GAPDH as an endogenous control. Data are presented as the mean ± SD (n = 3, each group). *p < 0.05 versus ZNF655⁺-NC group; #p < 0.05 versus ZNF655⁻-NC group.

the ZNF655-wild-type (WT) + LINC00346 group was significantly reduced compared with that in the ZNF655-WT + LINC00346-negative control (NC) group, whereas the luciferase activity in the ZNF655-mutant (Mut) groups were not affected (Figure 5A). However, the luciferase assays ZNF655-WT1 + LINC00346 did not influence the luciferase activity (Figures S2A and S2B). The results support the hypothesis that there is a putative-targeted combination between LINC00346 and ZNF655 mRNA 3′ UTR. RIP and RNA pull-down results further clarified the combination of LINC00346 and ZNF655 mRNA (Figures 5B and 5C). Furthermore, RIP results proved that LINC00346 and ZNF655 mRNA were both combined with STAU1 (Figures 5D and 5E). In addition, the half-life of ZNF655 mRNA was prolonged in GECs, respectively, treated with sh-LINC00346, STAU1⁻, or UPF1⁻ (Figures 5F–5H). Moreover, immunofluorescence staining was used to detect the observably highly expressed ZNF655 in the sh-LINC00346 group compared with the sh-NC group (Figure 5I). Then, we demonstrated that ZNF655 protein expression was significantly increased in the sh-LINC00346 group (Figure 5J). Besides, ZNF655 protein expres-

sion was significantly increased in the STAU1⁻ and UPF1⁻ group, respectively (Figures 5K and 5L). Moreover, ZNF655 protein exhibited a high expression, and the half-life of ZNF655 mRNA was dramatically prolonged in the sh-LINC00346 + STAU1⁻ group (Figures 5M and 5N).

LINC00346 Interacts with ZNF655 to Regulate the Angiogenesis of GECs

The results showed that the proliferation, migration, and tube formation of GECs were significantly increased in the pEX-LINC00346 + ZNF655⁻ group and decreased in the sh-LINC00346 + ZNF655⁺ group, whereas there were no significant changes in the pEX-LINC00346 + ZNF655⁺ group and sh-LINC00346 + ZNF655⁻ group (Figures 6A–6C). Besides, the EGFL7 and ROBO4 protein expression was significantly increased in the pEX-LINC00346 + ZNF655⁻ group and decreased in the sh-LINC00346 + ZNF655⁺ group, whereas there were no significant changes in the protein expression in the pEX-LINC00346 + ZNF655⁺ group and sh-LINC00346 + ZNF655⁻ group (Figures 6D and 6E).
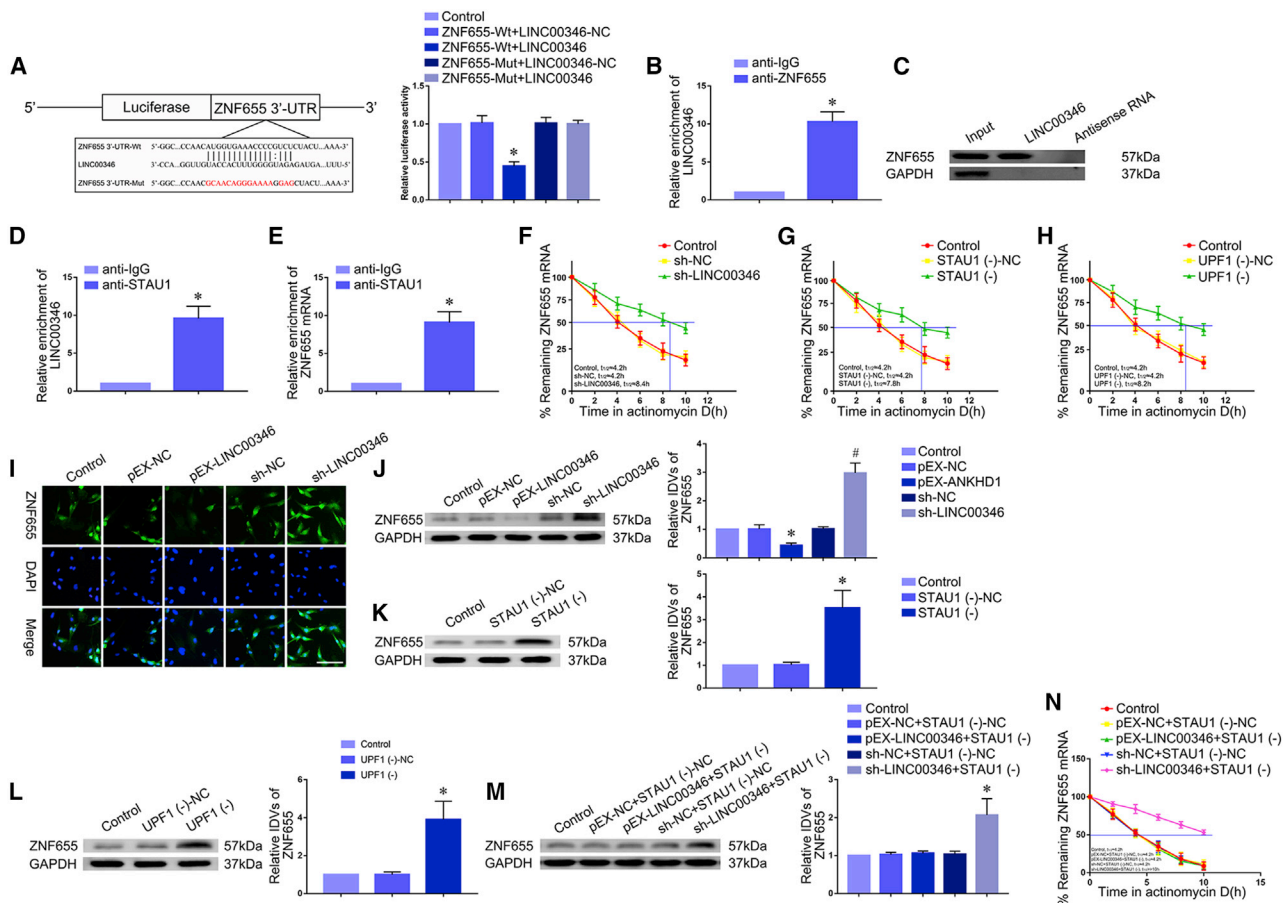
Figure 5. LINC00346 Combined with ZNF655 and Promoted the ZNF655 mRNA Degradation via SMD

(A) The predicted LINC00346 binding site in ZNF655 (ZNF655-WT) and/or the designed mutant sequence (ZNF655-Mut) were indicated. Luciferase reporter assay of HEK293T cells cotransfected with ZNF655-WT or ZNF655-Mut and LINC00346 or the LINC00346-NC. Data are presented as the mean ± SD (n = 3, each group). *p < 0.05 versus ZNF655-WT + LINC00346-NC group. (B) LINC00346 was identified in the ZNF655 complex. Relative enrichment of LINC00346 was measured using quantitative real-time PCR. Data are presented as the mean ± SD (n = 3, each group). *p < 0.05 versus anti-IgG group. (C) RNA pull-down determined that ZNF655 combined with LINC00346. ZNF655 and GAPDH protein levels in immunoprecipitation with LINC00346 were detected via western blots, and the expression levels of ZNF655 and GAPDH proteins were shown. (D and E) RIP assay confirmed that STAU1 bound to both LINC00346 (D) and ZNF655 (E). Relative enrichment of LINC00346 and ZNF655 mRNA was evaluated using quantitative real-time PCR. Data are presented as the mean ± SD (n = 3, each group). *p < 0.05 versus anti-IgG group. (F–H) The graphs, respectively, represented the different relative levels of the ZNF655 mRNA at the different actinomycin D treatment times. The groups were divided into the following: (F) control group, sh-NC group, and sh-LINC00346 group; (G) control group, STAU1⁻-NC group, and STAU1⁻ group; and (H) control group, UPF1⁻-NC group, and UPF1⁻ group. (I) Effect of LINC00346 on the expression of ZNF655 by immunofluorescence staining. ZNF655 (green) labeled with secondary antibody against ZNF655 antibody; nuclei (blue) are labeled with DAPI. Images are representative of 3 independent experiments. Scale bar, 30 μm. (J) Western blot analysis for LINC00346-regulated ZNF655 expression in GECs. (K) Western blot analysis for STAU1-regulated ZNF655 expression in GECs. (L) Western blot analysis for UPF1-regulated ZNF655 expression in GECs. (M) Western blot analysis for LINC00346 combined with STAU1-regulated ZNF655 expression in GECs. The relative IDVs of ZNF655 were shown using GAPDH as an endogenous control. Data are presented as the mean ± SD (n = 3, each group). (J) *p < 0.05 versus pEX-NC group; #p < 0.05 versus sh-NC group; (K) *p < 0.05 versus STAU1⁻-NC group; (L) *p < 0.05 versus UPF1⁻-NC group; and (M) *p < 0.05 versus sh-NC + STAU1⁻-NC group. (N) The graph represents the relative levels of the ZNF655 mRNA at the different actinomycin D treatment times in the control group, pEX-NC + STAU1⁻-NC group, pEX-LINC00346 + STAU1⁻ group, sh-NC + STAU1⁻-NC group, and sh-LINC00346 + STAU1⁻ group.

ZNF655 Inhibits ANKHD1 Expression via Targeting Its Promoter Region and Forms the ANKHD1/LINC00346/ZNF655 Feedback Loop

Chromatin immunoprecipitation (ChIP) assays were performed to verify whether ZNF655 could bind to the promoter region of EGFL7, ROBO4, and ANKHD1, respectively. With the search for bioinformatic database Wilmer Bioinformatics, we predicted a potential binding site within the promoter region of EGFL7, ROBO4, and ANKHD1, and the individual putative ZNF655 binding sites were identified by scanning the DNA sequence in the 2,000-bp region upstream and 200-bp region downstream of the transcription start site (TSS). In the meantime, we respectively amplified the 1,000-bp-upstream region of the individual putative ZNF655 binding sites on EGFL7, ROBO4, and ANKHD1 as the
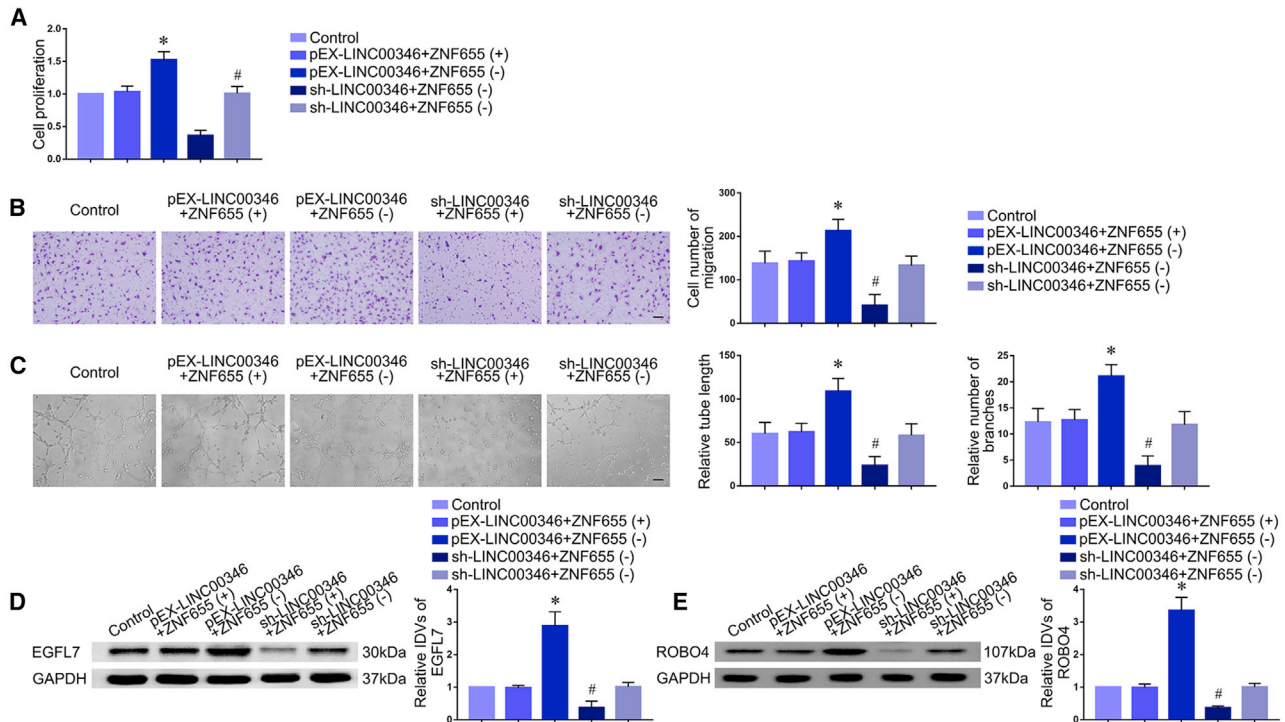
Figure 6. ZNF655 Reversed the Promotion Effect of LINC00346 in the Regulation of Angiogenesis of GECs

(A) A CCK-8 assay was conducted to evaluate the proliferation effect of LINC00346 and ZNF655 on GECs. (B) Transwell assay was used to measure the quantification number of migration cells with the expression of LINC00346 and ZNF655. (C) Matrigel tube formation assay was applied to determine the effect of LINC00346 and ZNF655 on the tube formation of GECs. Representative images and corresponding statistical plots are presented. Data are presented as the mean ± SD (n = 3, each group). *p < 0.05 versus control group; #p < 0.05 versus control group. Scale bars, 30 μm. (D and E) Western blot analysis for LINC00346 bound to ZNF655-regulated EGFL7 (D) and ROBO4 (E) expression in GECs. The relative IDVs of EGFL7 and ROBO4 were shown using GAPDH as an endogenous control. Data are presented as the mean ± SD (n = 3, each group). *p < 0.05 versus control group; #p < 0.05 versus control group.

corresponding negative control. The results demonstrated that there was a direct association of ZNF655 with the putative binding site of EGFL7, the putative binding site of ROBO4, and the putative binding site of ANKHD1, respectively, whereas there was no association of ZNF655 with all of the control regions (Figures 7A–7C). Also, we used quantitative real-time PCR to, respectively, detect the relative DNA enrichment of EGFL7, ROBO4, and, ANKHD1 (Figure 7D). Meanwhile, luciferase reporter assays verified that ZNF655 inhibited the transcription of EGFL7, ROBO4, and ANKHD1 by binding to their promoter region, respectively (Figures 7E–7G). In addition, EGFL7, ROBO4, and ANKHD1 mRNA expression was significantly decreased in the ZNF655^{+} group compared with the ZNF655^{+}-NC group, whereas the opposite results were shown in the ZNF655^{−} group (Figures 7H–7J). Besides, overexpression of ZNF655 significantly decreased ANKHD1 protein expression (Figure 7K). Further, ZNF655 protein expression was significantly decreased in the pEX-ANKHD1 group, whereas inhibition of ANKHD1 led to a marked increase (Figure 7L). Also, there were no significant changes in the protein expression of ZNF655 in the pEX-ANKHD1 + sh-LINC00346 group and sh-ANKHD1 + pEX-LINC00346 group (Figure 7M).

Knockdown of ANKHD1 and LINC00346 Combined with Overexpression of ZNF655 Restrains Glioma Angiogenesis *In Vivo*

Matrigel plug assay was conducted to further evaluate the glioma angiogenesis *in vivo*. As shown in Figures 8A and 8B, the amount of hemoglobin in the sh-ANKHD1 group, sh-LINC00346 group, ZNF655^{+} group, and sh-ANKHD1 + sh-LINC00346 + ZNF655^{+} group was significantly decreased compared with the control group. At the same time, the amount of hemoglobin in the sh-ANKHD1 + sh-LINC00346 + ZNF655^{+} group exerted a marked decrease compared with the sh-ANKHD1 group, sh-LINC00346 group, and ZNF655^{+} group, respectively. These results demonstrate that with the combination of ANKHD1 knockdown, LINC00346 knockdown, and ZNF655 overexpression present, the more prominent inhibitory effect on glioma angiogenesis *in vivo*.

DISCUSSION

In this study, we demonstrated that ANKHD1 was upregulated in GECs. The knockdown of ANKHD1 impeded the GEC proliferation, migration, and tube formation. ANKHD1 enhanced the stability of LINC00346 and increased its expression. Inhibition of ANKHD1
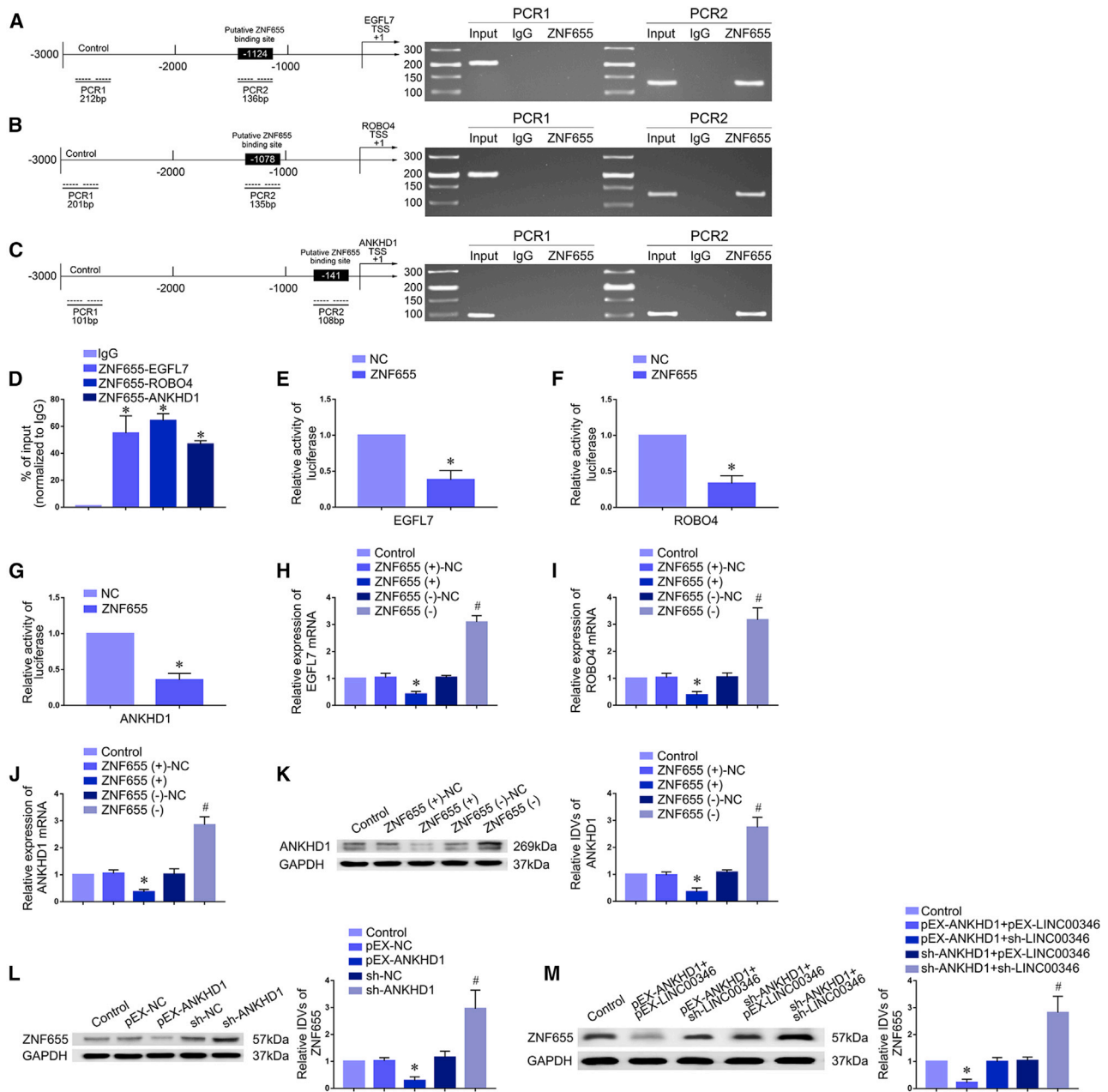
Figure 7. ZNF655, Respectively, Bound to the Promoter of Target Genes and Exerted the Transcriptional Inhibitory Role

(A–C) ZNF655 targeted the promoters of EGFL7 (A), ROBO4 (B), and ANKHD1 (C) in GECs, respectively. Each transcription start site (TSS) was designated as +1. Putative ZNF655 binding sites are illustrated, respectively. Immunoprecipitated DNA was amplified by PCR. Normal rabbit IgG was used as a negative control. (D) Quantitative real-time PCR analysis for the enrichment value of ZNF655 immunoprecipitated chromatin was calculated by IgG immunoprecipitated chromatin as a negative control. Data are presented as the mean ± SD (n = 3, each group). *p < 0.05 versus IgG group. (E–G) Luciferase reporter assays were conducted to detect the combination between ZNF655 and the target gene EGFL7 (E), ROBO4 (F), and ANKHD1 (G) promoter, respectively. Data are presented as the mean ± SD (n = 3, each group). *p < 0.05 versus NC group. (H–J) Quantitative real-time PCR for ZNF655, respectively, regulated EGFL7 (H), ROBO4 (I), and ANKHD1 (J) mRNA expression in GECs. Each of the relative expressions of EGFL7, ROBO4, and ANKHD1 mRNA in GECs was shown using GAPDH as an endogenous control. Data are presented as the mean ± SD (n = 3, each group). *p < 0.05 versus ZNF655^{+}-NC group; #p < 0.05 versus ZNF655^{−}-NC group. (K) Western blot analysis for ZNF655-regulated ANKHD1 expression in GECs. The relative IDV of ANKHD1 was shown using GAPDH as an endogenous control. Data are presented as the mean ± SD (n = 3, each group). *p < 0.05 versus ZNF655^{+}-NC group; #p < 0.05 versus ZNF655^{−}-NC group. (L) Western blot analysis for ANKHD1-regulated ZNF655 expression in GECs. The relative IDV of ZNF655 was shown using GAPDH as an endogenous control. Data are presented as the mean ± SD (n = 3, each group). *p < 0.05 versus pEX-NC group; #p < 0.05 versus sh-NC group. (M) Western blot analysis for ANKHD1

(legend continued on next page)

shortened the half-life of LINC00346, which was normally expressed at high levels in GECs. The knockdown of LINC00346 inhibited the angiogenesis of GECs. In addition, ANKHD1 targeted LINC00346, and overexpression of LINC00346 reversed the inhibitory effect of silencing ANKHD1 in the regulation of glioma angiogenesis. ZNF655 exhibited low expression levels in GECs. ZNF655 overexpression suppressed GEC proliferation, migration, and tube formation. LINC00346 specifically bound to ZNF655 mRNA via their Alu elements. Furthermore, we found that LINC00346 facilitated the degradation of ZNF655 mRNA via SMD and regulated the angiogenesis of GECs. Moreover, ZNF655 targeted the promoter region of ANKHD1, inhibited transcription, and formed an ANKHD1/LINC00346/ZNF655 feedback loop that regulated glioma angiogenesis.

In the present study, we found, for the first time, that ANKHD1 was expressed at high levels in GECs. Recent studies have indicated that RBPs play a role in regulating tumor development. For example, SRSF6 is upregulated in colorectal cancer (CRC) samples and cell lines. High SRSF6 expression promotes CRC cell proliferation metastasis *in vitro* and *in vivo*.[25] ANKHD1 is highly expressed in human prostate and breast cancer and significantly reduces patient survival time.[26,27] However, the function of ANKHD1 in glioma and in regulating GECs is still unclear. In this study, inhibition of ANKHD1 significantly suppressed the proliferation, migration, and tube formation of GECs and reduced the expression of EGFL7 and ROBO4, which are the biomarkers of tumor angiogenesis. This indicated that ANKHD1 promoted angiogenesis of GECs. The above research results indicate that ANKHD1, which is highly expressed in GECs, plays an oncogenic role in regulating angiogenesis of glioma.

Further, we explored the target genes that were directly regulated by ANKHD1. The microarray analysis results showed that LINC00346 was significantly decreased in GECs after downregulation of ANKHD1. Accumulating evidence has demonstrated that lncRNA is abnormally expressed in many malignant tumors and serves as a molecular marker in the diagnosis and treatment of cancer.[28–30] Studies have shown that the upregulated expression of LINC00346 in non-small cell lung cancer promotes the cell proliferation, whereas inhibits the apoptosis.[31] However, there has not been any research about the expression and function of LINC00346 in glioma angiogenesis. The results from The Cancer Genome Atlas (TCGA) database analysis indicated that LINC00346 is highly expressed in glioma tissues, and the expression of LINC00346 is significantly, positively correlated with the poor prognosis of glioma patients. In this study, we found that LINC00346 was also highly expressed in GECs. The knockdown of LINC00346 inhibited GEC proliferation, migration, and tube formation. Our results suggest that LINC00346 acts as an oncogene in glioma, and inhibition of LINC00346 may abrogate glioma angiogenesis. In the meantime, we detected that knockdown of ANKHD1 significantly inhibited the expression of LINC00346 in

GECs. Thus, the above results indicated that ANKHD1 facilitated glioma angiogenesis by regulating LINC00346. However, the molecular mechanism by which ANKHD1 regulates LINC00346 during the angiogenesis associated with glioma is still unclear; therefore, the specific mechanism has attracted our attention.

In the present study, we demonstrated that the silencing of ANKHD1 in GECs significantly reduced the half-life of LINC00346, but there was no significant difference for the relative expression of nascent LINC00346 in pEX-ANKHD1. With the use of RBPmap bioinformatics software, we detected a binding site between ANKHD1 and LINC00346. Meanwhile, RIP results revealed that ANKHD1 bound to LINC00346. The biological role of this complex is carried out through its binding to the Ago2 protein of the RNA-induced silencing complex (RISC). These exploratory findings indicate that ANKHD1 promotes the expression of LINC00346 by increasing the stability of LINC00346. Studies have shown that RBP dysregulation, which regulates several vital processes, such as splicing and translation of lncRNAs, enhances the stability of lncRNAs, increasing lncRNAs expression, and regulates the malignant behavior of tumors.[32,33] Furthermore, we detected that there were no significant changes in GEC proliferation, migration, and tube formation following overexpression of ANKHD1 combined with inhibition of LINC00346 or inhibition of ANKHD1 combined with overexpression of LINC00346. These indicated that there was a reversing effect between ANKHD1 and LINC00346 in regulating the angiogenesis of GECs. Together, the above results suggest that ANKHD1 plays a role in the regulation of glioma angiogenesis by targeting LINC00346 and enhancing its stability.

We further explored the target gene ZNF655 regulated by LINC00346 via microarray analysis. Our findings indicated that ZNF655 was expressed at low levels in GECs. Overexpression of ZNF655 significantly inhibited GEC proliferation, migration, and tube formation, which indicated that ZNF655 inhibited glioma angiogenesis. In addition, knockdown of LINC00346 in GECs notably increased the expression of ZNF655. Therefore, the regulatory mechanism of LINC00346 on the target gene ZNF655 has aroused our interest. Furthermore, we explored that inhibition of LINC00346 increased the half-life of ZNF655 mRNA. These results fully show that LINC00346 can reduce the stability of ZNF655 and promote its mRNA degradation.

We further investigated the mechanism by which LINC00346 promoted the degradation of ZNF655 mRNA. Recent studies show that the SMD mechanism plays a role in the regulation of mRNA degradation mediated by STAU1. STAU1 regulates mRNA degradation by binding to the SBS of target mRNA 3′ UTR.[34–36] The formation of the SBS can be divided into two types: (1) intramolecular base pairing through the 3′ UTR of the target mRNA or the Alu element in the 3′ UTR of the target mRNA and (2) specific recognition and pairing of the Alu element between lncRNAs and the 3′ UTR of the target

combined with LINC00346-regulated ZNF655 expression in GECs. The relative IDV of ZNF655 was shown using GAPDH as an endogenous control. Data are presented as the mean ± SD (n = 3, each group). *p < 0.05 versus control group; #p < 0.05 versus control group.
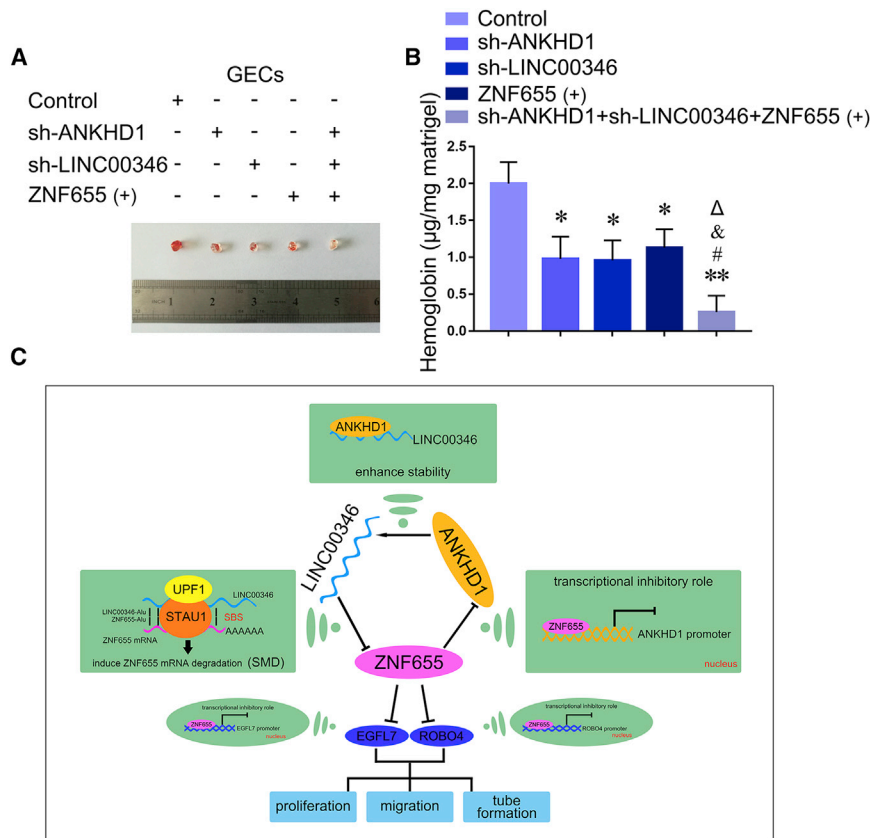
Figure 8. ANKHD1 and LINC00346 Knockdown Combined with ZNF655 Overexpression Suppressed Glioma Angiogenesis *In Vivo*

(A) The coeffect of ANKHD1, LINC00346, and ZNF655 on the glioma angiogenesis *in vivo* was detected by Matrigel plug assay. (B) The amount of hemoglobin was evaluated after the combination of ANKHD1, LINC00346, and ZNF655. Data are presented as the mean ± SD (n = 3, each group). *p < 0.05 versus control group; #p < 0.05 versus sh-ANKHD1 group; &p < 0.05 versus sh-LINC00346 group; Δp < 0.05 versus ZNF655 (+) group. (C) Schematic illustration of the mechanism of the ANKHD1/LINC00346/ZNF655 feedback loop in the regulation of glioma angiogenesis.

mary, we explored that LINC00346 can mediate the degradation of ZNF655 mRNA via SMD, thereby promoting glioma angiogenesis.

Previous studies have indicated that transcription factors regulate target gene expression by binding to their promoters. TEAD4 increases the expression of A3B by binding to its promoter in esophageal cancer cells.[41] SNAI1 binds to the promoter of E-cadherin and inhibits its transcription in breast cancer cells.[42] With the use of the Wilmer Bioinformatics database, we identified a potential binding site within the promoter region of EGFL7, ROBO4, and ANKHD1 for the transcription factor ZNF655. Furthermore, ChIP assays confirmed that ZNF655 directly bound to a specific sequence in the promoters of these three genes. In addition, luciferase reporter assays showed that ZNF655 markedly reduced the EGFL7, ROBO4, and ANKHD1 promoter activity. Furthermore, ZNF655 overexpression led to decreased EGFL7, ROBO4, and ANKHD1 mRNA and protein expression levels. These results demonstrated that ZNF655 has a transcriptional inhibitory role, which decreased the expression of ANKHD1 in GECs. In this study, we also determined that the inhibition of ANKHD1 or the simultaneous inhibition of ANKHD1 and LINC00346 significantly upregulated ZNF655 expression. Thus, ZNF655 is part of an ANKHD1/LINC00346/ZNF655 feedback loop, which plays an important role in the regulation of glioma angiogenesis. The mechanism is schematically presented in Figure 8C.

Finally, we measured the ability of glioma angiogenesis *in vivo* using a Matrigel plug assay. Accumulating evidence shows that the Matrigel plug assay can reflect the ability of angiogenesis *in vivo*.[43,44] Thus, in our research, it will be interesting to explore the use of an ANKHD1 or LINC00346 inhibitor, a ZNF655 agonist, or their combination as potential therapeutic agents against glioma.

In summary, the present study is the first demonstration of endogenous expression of ANKHD1, LINC00346, and ZNF655 in GECs. Then we detected the interactions among ANKHD1, LINC00346, and ZNF655

mRNA.[37–39] For example, HOXA11-AS promotes KLF2 mRNA degradation via SMD, which regulates the cell cycle and metastasis of gastric cancer cells.[40] In this study, we used RepeatMasker software to determine whether Alu elements were present in both LINC00346 and 3′ UTR of ZNF655 mRNA. At the same time, we used IntaRNA software to predict the base-pairing sequence between LINC00346 and ZNF655 mRNA 3′ UTR. Furthermore, dual-luciferase gene reporter assays were conducted to verify the interaction between LINC00346 and ZNF655 mRNA via their Alu elements and confirm that ZNF655 is a target of LINC00346. In addition, RIP and RNA pull-down results demonstrated that LINC00346 and ZNF655 mRNA were both bound to STAU1. Moreover, knockdown of STAU1 and UPF1 significantly upregulated ZNF655 protein levels and prolonged the ZNF655 mRNA half-life. In the meanwhile, we demonstrated that knockdown of STAU1 reversed the effect of overexpression of LINC00346 on ZNF655 protein expression and half-life of ZNF655 mRNA. The above results indicated that LINC00346 and ZNF655 mRNA were specifically recognized and paired through their Alu elements, which formed an SBS to bind to STAU1. STAU1 recruited and bound to UPF1, which triggered ZNF655 mRNA degradation through SMD and regulated glioma angiogenesis. Furthermore, the results showed that simultaneous overexpression or inhibition of LINC00346 and ZNF655 caused no significant alteration in the proliferation, migration, and tube formation of GECs. These results showed that ZNF655 could reverse the promotion effect of LINC00346 in the regulation of glioma angiogenesis. In sum-

in GECs. Our exploratory study found that ANKHD1 binds and enhances the stability of LINC00346 and upregulates its expression. Meanwhile, LINC00346 mediates the degradation of ZNF655 mRNA via SMD. Further, ZNF655 directly binds to the ANKHD1 promoter region and exerts a transcriptional repression effect so that we identified an ANKHD1/LINC00346/ZNF655 feedback loop in the regulation of glioma angiogenesis. In this study, we examined that the innovative molecular network formed by ANKHD1, LINC00346, ZNF655, EGFL7, and ROBO4 regulates glioma angiogenesis from multiple dimensions by detecting expression levels, investigating cell functions, analyzing interactions between target genes, and verifying at the *in vivo* level. The results of this study provide new theoretical and experimental evidence for the development of glioma and new targets and strategies for anti-angiogenesis therapy against glioma.

MATERIALS AND METHODS

Cell Culture
Human glioblastoma cell line U87 and human embryonic kidney 293T (HEK293T) cells were purchased from Shanghai Institutes for Biological Sciences Cell Resource Center. Primary normal human astrocytes (NHAs) were purchased from the ScienCell Research Laboratories (Carlsbad, CA, USA), and the immortalized human cerebral microvascular EC line hCMEC/D3 was acquired from Dr. Couraud (Institute Cochin, Paris, France). Glioma conditioned medium was obtained from the U87 glioblastoma cells, and the ECs and astrocytes conditioned medium were obtained from the NHA cells and the ECs. We cultured U87 cells, HEK293T cells, NHA cells, and ECs and obtained glioma conditioned medium and astrocytes conditioned medium as previously described.[45] For details, see Supplemental Materials and Methods. Then we got the GECs for the subsequent experiments.

FISH
FISH assays were performed as previously described.[46] For identification of ANKHD1, LINC00346, and ZNF655 rearrangement in GECs, the ANKHD1 probe (green-labeled; ShineGene Molecular Biotech, Shanghai, China), LINC00346 probe (green-labeled; GenePharma, Shanghai, China), and ZNF655 probe (green-labeled; ShineGene Molecular Biotech, Shanghai, China) were used. Also see Supplemental Materials and Methods for details.

Quantitative Real-Time PCR
Total RNA was extracted from AECs and GECs using Trizol reagent (Life Technologies, Carlsbad, CA, USA). See Supplemental Materials and Methods for details.

Human lncRNA and mRNA Microarray Analysis
For the lncRNA and mRNA analysis, sample preparation and microarray hybridization were performed by Kangchen Bio-tech (Shanghai, China).

Plasmid Construction and Cell Transfection
Plasmid construction and cell transfection were performed as previously described.[46] For details, see Supplemental Materials and Methods.

Cell Proliferation Assay
CCK-8 assay (Dojin, Japan) was conducted to detect the proliferation of GECs. For details, also see Supplemental Materials and Methods.

Cell Migration Assay
The migration of GECs *in vitro* was determined using the 24-well chambers with an 8-mm pore size (Corning, USA). Also see Supplemental Materials and Methods for details.

Tube Formation Assay
Matrigel tube formation assay was performed to evaluate endothelial tube formation *in vitro* as previously described.[45] For details, see Supplemental Materials and Methods.

Western Blot Analysis
Western blot was performed as previously described.[46] For details and antibodies used, see Supplemental Materials and Methods.

Nucleus-Cytoplasm Separation Assay
The nucleus and cytoplasm fractions of GECs were separated by using the RNA and protein isolation (PARIS) Kit (Invitrogen, Carlsbad, CA, USA). The extracted lysates of nucleus and cytoplasm were stored at −80°C for further study. The RNA and protein in the nucleus and cytoplasm of GECs were extracted. Further, ANKHD1 mRNA, LINC00346, and ZNF655 mRNA were detected by quantitative real-time PCR. ANKHD1 and ZNF655 protein were detected by western blot. For details, see Supplemental Materials and Methods.

Immunofluorescence Assay
Immunofluorescence assay was performed as previously described.[47] For details and antibodies used, see Supplemental Materials and Methods.

Reporter Vector Constructs and Luciferase Reporter Assay
The putative LINC00346 binding site of the ZNF655 3′ UTR sequence and the respective putative ZNF655 mRNA binding site of EGFL7, ROBO4, and ANKHD1 mRNA were amplified by PCR and cloned into a pmirGLO Dual-Luciferase Target Expression Vector (Promega, Madison, WI, USA) to construct a luciferase reporter vector (GenePharma). Luciferase assays were performed as previously described.[46] Also see Supplemental Materials and Methods for details.

RIP
RIP assay was conducted as previously reported.[46] See Supplemental Materials and Methods for details.

RNA Pull-Down
RNA pull-down assay was performed as previously described.[46] Also see Supplemental Materials and Methods for details.

RNA Stability Measurement
RNA stability measurement was conducted as previously described.[46] See Supplemental Materials and Methods for details. Actinomycin D (5 mg/mL final concentration) was used to treat the transfected and

untransfected cells as control and then, respectively, we collected the total RNA of target genes at different time points and analyzed their half-life using quantitative real-time PCR.

Click-iT Capture Nascent RNA
Click-iT Nascent RNA Capture Kit (Invitrogen) was conducted to label and capture newly synthesized RNA as previously reported.[48] In brief, 5-ethymyl uridine (EU) was used to label the newly synthesized RNA, and streptavidin magnetic beads were conducted to isolate the nascent RNA. Then we used quantitative real-time PCR to detect the expression of the nascent RNA.

ChIP Assay
The SimpleChIP Enzymatic Chromatin IP Kit (Cell Signaling Technology, Danvers, MA, USA) was used for ChIP assays, according to the instructions provided by the manufacturer. In a nutshell, cells were crosslinked with 1% formaldehyde. The lysis buffer was used to lyse the cells, and then the micrococcal nuclease was used to digest the chromatin. Immunoprecipitates were incubated with 3 μg of anti-ZNF655 or normal rabbit IgG, followed by immunoprecipitating with Protein G agarose beads at 4°C with gentle shaking overnight. 2% aliquots of lysates were used as an input control and stored at −20°C. 5 M NaCl and proteinase K were used to reverse the DNA crosslink, and the ChIP DNA was finally purified. Immunoprecipitated DNA was amplified by PCR using the specific primers (as Table S1). ChIP-qPCR analysis of DNA immunoprecipitated was used to quantify the relative DNA enrichment. Thermocycling conditions were 95°C for 3 min (enzyme activation), followed by 40 cycles at 95°C for 15 s and 60°C for 30 s. The enrichment percentage of DNA enrichment was calculated by $2\% \times 2^{(C[T]\text{input sample} - C[T]\text{IP sample})}$ method, where C[T] is threshold cycle of PCR reaction.

In Vivo Matrigel Plug Assay
The Matrigel plug assay was used to evaluate the glioma angiogenesis as previously described.[45] For details, see Supplemental Materials and Methods.

Statistical Analysis
Data are presented as mean ± standard deviation (SD). SPSS 22.0 statistical software (IBM, New York, NY, USA) with the Student's t test or one-way analysis of variance, followed by Bonferroni's post-test, was used to measure all statistical analyses. Differences were considered to be significant when p <0.05.

SUPPLEMENTAL INFORMATION
Supplemental Information can be found online at https://doi.org/10.1016/j.omtn.2020.05.004.

AUTHOR CONTRIBUTIONS
Y.L. and C.Y. contributed to the experiment design, implementation, manuscript draft, and data analysis. J.Z. and X.L. contributed to the experiment implementation and data analysis. Y.X. conceived or designed the experiments. C.Y., Q.H., Y.D., and D.W. performed the experiments. Z.L., L.L., J.M., and H.C. analyzed the data. C.Y. conceived or designed the experiments, performed the experiments, and wrote the manuscript. All authors read and approved the final manuscript.

CONFLICTS OF INTEREST
The authors declare no competing interests.

ACKNOWLEDGMENTS

REFERENCES
1. Zepecki, J.P., Snyder, K.M., Moreno, M.M., Fajardo, E., Fiser, A., Ness, J., Sarkar, A., Toms, S.A., and Tapinos, N. (2019). Regulation of human glioma cell migration, tumor growth, and stemness gene expression using a Lck targeted inhibitor. Oncogene 38, 1734–1750.

2. Laszlo, V., Valko, Z., Kovacs, I., Ozsvar, J., Hoda, M.A., Klikovits, T., Lakatos, D., Czirok, A., Garay, T., Stiglbauer, A., et al. (2018). Nintedanib Is Active in Malignant Pleural Mesothelioma Cell Models and Inhibits Angiogenesis and Tumor Growth *In Vivo*. Clin. Cancer Res. 24, 3729–3740.

3. Boyd, N.H., Walker, K., Ayokanmbi, A., Gordon, E.R., Whetsel, J., Smith, C.M., Sanchez, R.G., Lubin, F.D., Chakraborty, A., Tran, A.N., et al. (2019). Chromodomain Helicase DNA-Binding Protein 7 Is Suppressed in the Perinecrotic/Ischemic Microenvironment and Is a Novel Regulator of Glioblastoma Angiogenesis. Stem Cells 37, 453–462.

4. Banerjee, A., Vest, K.E., Pavlath, G.K., and Corbett, A.H. (2017). Nuclear poly(A) binding protein 1 (PABPN1) and Matrin3 interact in muscle cells and regulate RNA processing. Nucleic Acids Res. 45, 10706–10725.

5. de Silva, H.C., Lin, M.Z., Phillips, L., Martin, J.L., and Baxter, R.C. (2019). IGFBP-3 interacts with NONO and SFPQ in PARP-dependent DNA damage repair in triple-negative breast cancer. Cell. Mol. Life Sci. 76, 2015–2030.

6. Yu, X., Zheng, H., Chan, M.T.V., and Wu, W.K.K. (2018). NOVA1 acts as an oncogene in melanoma via regulating FOXO3a expression. J. Cell. Mol. Med. 22, 2622–2630.

7. Zong, F.Y., Fu, X., Wei, W.J., Luo, Y.G., Heiner, M., Cao, L.J., Fang, Z., Fang, R., Lu, D., Ji, H., and Hui, J. (2014). The RNA-binding protein QKI suppresses cancer-associated aberrant splicing. PLoS Genet. 10, e1004289.

8. Machado-Neto, J.A., Lazarini, M., Favaro, P., de Melo Campos, P., Scopim-Ribeiro, R., Franchi Junior, G.C., Nowill, A.E., Lima, P.R., Costa, F.F., Benichou, S., et al. (2015). ANKHD1 silencing inhibits Stathmin 1 activity, cell proliferation and migration of leukemia cells. Biochim. Biophys. Acta 1853, 583–593.

9. Dhyani, A., Duarte, A.S., Machado-Neto, J.A., Favaro, P., Ortega, M.M., and Olalla Saad, S.T. (2012). ANKHD1 regulates cell cycle progression and proliferation in multiple myeloma cells. FEBS Lett. 586, 4311–4318.

10. Dhyani, A., Machado-Neto, J.A., Favaro, P., and Saad, S.T. (2015). ANKHD1 represses p21 (WAF1/CIP1) promoter and promotes multiple myeloma cell growth. Eur. J. Cancer 51, 252–259.

11. Mishra, S., Verma, S.S., Rai, V., Awasthee, N., Chava, S., Hui, K.M., Kumar, A.P., Challagundla, K.B., Sethi, G., and Gupta, S.C. (2019). Long non-coding RNAs are emerging targets of phytochemicals for cancer and other chronic diseases. Cell. Mol. Life Sci. 76, 1947–1966.

12. Tran, D.D.H., Kessler, C., Niehus, S.E., Mahnkopf, M., Koch, A., and Tamura, T. (2018). Myc target gene, long intergenic noncoding RNA, Linc00176 in hepatocellular carcinoma regulates cell cycle and cell survival by titrating tumor suppressor microRNAs. Oncogene 37, 75–85.

13. Li, W., Dou, Z., We, S., Zhu, Z., Pan, D., Jia, Z., Liu, H., Wang, X., and Yu, G. (2018). Long noncoding RNA BDNF-AS is associated with clinical outcomes and has functional role in human prostate cancer. Biomed. Pharmacother. 102, 1105–1110.

14. Ye, T., Ding, W., Wang, N., Huang, H., Pan, Y., and Wei, A. (2017). Long noncoding RNA linc00346 promotes the malignant phenotypes of bladder cancer. Biochem. Biophys. Res. Commun. 491, 79–84.

15. Cho, H., Kim, K.M., Han, S., Choe, J., Park, S.G., Choi, S.S., and Kim, Y.K. (2012). Staufen1-mediated mRNA decay functions in adipogenesis. Mol. Cell 46, 495–506.

16. Cho, H., Han, S., Park, O.H., and Kim, Y.K. (2013). SMG1 regulates adipogenesis via targeting of staufen1-mediated mRNA decay. Biochim. Biophys. Acta 1829, 1276–1287.

17. Kim, M.Y., Park, J., Lee, J.J., Ha, D.H., Kim, J., Kim, C.G., Hwang, J., and Kim, C.G. (2014). Staufen1-mediated mRNA decay induces Requiem mRNA decay through binding of Staufen1 to the Requiem 3′UTR. Nucleic Acids Res. 42, 6999–7011.

18. Jolly, L.A., Homan, C.C., Jacob, R., Barry, S., and Gecz, J. (2013). The UPF3B gene, implicated in intellectual disability, autism, ADHD and childhood onset schizophrenia regulates neural progenitor cell behaviour and neuronal outgrowth. Hum. Mol. Genet. 22, 4673–4687.

19. Houlard, M., Romero-Portillo, F., Germani, A., Depaux, A., Regnier-Ricard, F., Gisselbrecht, S., and Varin-Blank, N. (2005). Characterization of VIK-1: a new Vav-interacting Kruppel-like protein. Oncogene 24, 28–38.

20. Yamauchi, M., Fukuda, T., Wada, T., Kawanishi, M., Imai, K., Tasaka, R., Yasui, T., and Sumi, T. (2016). Expression of epidermal growth factor-like domain 7 may be a predictive marker of the effect of neoadjuvant chemotherapy for locally advanced uterine cervical cancer. Oncol. Lett. 12, 5183–5189.

21. Shen, X., Han, Y., Xue, X., Li, W., Guo, X., Li, P., Wang, Y., Li, D., Zhou, J., and Zhi, Q. (2016). Epidermal growth factor-like domain 7 promotes cell invasion and angiogenesis in pancreatic carcinoma. Biomed. Pharmacother. 77, 167–175.

22. Zhao, H., Ahirwar, D.K., Oghumu, S., Wilkie, T., Powell, C.A., Nasser, M.W., Satoskar, A.R., Li, D.Y., and Ganju, R.K. (2016). Endothelial Robo4 suppresses breast cancer growth and metastasis through regulation of tumor angiogenesis. Mol. Oncol. 10, 272–281.

23. Wang, F.Y., Kang, C.S., Wang-Gou, S.Y., Huang, C.H., Feng, C.Y., and Li, X.J. (2017). EGFL7 is an intercellular EGFR signal messenger that plays an oncogenic role in glioma. Cancer Lett. 384, 9–18.

24. Cai, H., Xue, Y., Li, Z., Hu, Y., Wang, Z., Liu, W., Li, Z., and Liu, Y. (2015). Roundabout4 suppresses glioma-induced endothelial cell proliferation, migration and tube formation in vitro by inhibiting VEGR2-mediated PI3K/AKT and FAK signaling pathways. Cell. Physiol. Biochem. 35, 1689–1705.

25. Wan, L., Yu, W., Shen, E., Sun, W., Liu, Y., Kong, J., Wu, Y., Han, F., Zhang, L., Yu, T., et al. (2019). SRSF6-regulated alternative splicing that promotes tumour progression offers a therapy target for colorectal cancer. Gut 68, 118–129.

26. Machado-Neto, J.A., Lazarini, M., Favaro, P., Franchi, G.C., Jr., Nowill, A.E., Saad, S.T., and Traina, F. (2014). ANKHD1, a novel component of the Hippo signaling pathway, promotes YAP1 activation and cell cycle progression in prostate cancer cells. Exp. Cell Res. 324, 137–145.

27. Sansores-Garcia, L., Atkins, M., Moya, I.M., Shahmoradgoli, M., Tao, C., Mills, G.B., and Halder, G. (2013). Mask is required for the activity of the Hippo pathway effector Yki/YAP. Curr. Biol. 23, 229–235.

28. Xu, T., Yan, S., Jiang, L., Yu, S., Lei, T., Yang, D., Lu, B., Wei, C., Zhang, E., and Wang, Z. (2019). Gene Amplification-Driven Long Noncoding RNA SNHG17 Regulates Cell Proliferation and Migration in Human Non-Small-Cell Lung Cancer. Mol. Ther. Nucleic Acids 17, 405–413.

29. Tiessen, I., Abildgaard, M.H., Lubas, M., Gylling, H.M., Steinhauer, C., Pietras, E.J., Diederichs, S., Frankel, L.B., and Lund, A.H. (2019). A high-throughput screen identifies the long non-coding RNA DRAIC as a regulator of autophagy. Oncogene 38, 5127–5141.

30. Dolcino, M., Tinazzi, E., Puccetti, A., and Lunardi, C. (2019). In Systemic Sclerosis, a Unique Long Non Coding RNA Regulates Genes and Pathways Involved in the Three Main Features of the Disease (Vasculopathy, Fibrosis and Autoimmunity) and in Carcinogenesis. J. Clin. Med. 8, 320.

31. Wang, F., Chen, J.G., Wang, L.L., Yan, Z.Z., Chen, S.P., and Wang, X.G. (2017). Up-regulation of LINC00346 inhibits proliferation of non-small cell lung cancer cells through mediating JAK-STAT3 signaling pathway. Eur. Rev. Med. Pharmacol. Sci. 21, 5135–5142.

32. Tichon, A., Perry, R.B., Stojic, L., and Ulitsky, I. (2018). SAM68 is required for regulation of Pumilio by the NORAD long noncoding RNA. Genes Dev. 32, 70–78.

33. Liu, X., Zheng, J., Xue, Y., Qu, C., Chen, J., Wang, Z., Li, Z., Zhang, L., and Liu, Y. (2018). Inhibition of TDP43-Mediated SNHG12-miR-195-SOX5 Feedback Loop Impeded Malignant Biological Behaviors of Glioma Cells. Mol. Ther. Nucleic Acids 10, 142–158.

34. Gong, C., Tang, Y., and Maquat, L.E. (2013). mRNA-mRNA duplexes that autoelicit Staufen1-mediated mRNA decay. Nat. Struct. Mol. Biol. 20, 1214–1220.

35. Sakurai, M., Shiromoto, Y., Ota, H., Song, C., Kossenkov, A.V., Wickramasinghe, J., Showe, L.C., Skordalakes, E., Tang, H.Y., Speicher, D.W., and Nishikura, K. (2017). ADAR1 controls apoptosis of stressed cells by inhibiting Staufen1-mediated mRNA decay. Nat. Struct. Mol. Biol. 24, 534–543.

36. Park, E., Gleghorn, M.L., and Maquat, L.E. (2013). Staufen2 functions in Staufen1-mediated mRNA decay by binding to itself and its paralog and promoting UPF1 helicase but not ATPase activity. Proc. Natl. Acad. Sci. USA 110, 405–412.

37. Wang, J., Gong, C., and Maquat, L.E. (2013). Control of myogenesis by rodent SINE-containing lncRNAs. Genes Dev. 27, 793–804.

38. Gong, C., and Maquat, L.E. (2011). lncRNAs transactivate STAU1-mediated mRNA decay by duplexing with 3′ UTRs via Alu elements. Nature 470, 284–288.

39. Lucas, B.A., Lavi, E., Shiue, L., Cho, H., Katzman, S., Miyoshi, K., Siomi, M.C., Carmel, L., Ares, M., Jr., and Maquat, L.E. (2018). Evidence for convergent evolution of SINE-directed Staufen-mediated mRNA decay. Proc. Natl. Acad. Sci. USA 115, 968–973.

40. Liu, Z., Chen, Z., Fan, R., Jiang, B., Chen, X., Chen, Q., Nie, F., Lu, K., and Sun, M. (2017). Over-expressed long noncoding RNA HOXA11-AS promotes cell cycle progression and metastasis in gastric cancer. Mol. Cancer 16, 82.

41. Mori, S., Takeuchi, T., Ishii, Y., Yugawa, T., Kiyono, T., Nishina, H., and Kukimoto, I. (2017). Human Papillomavirus 16 E6 Upregulates APOBEC3B via the TEAD Transcription Factor. J. Virol. 91, e02413–e02416.

42. Lu, Y., Yu, L., Yang, M., Jin, X., Liu, Z., Zhang, X., Wang, L., Lin, D., Liu, Y., Wang, M., and Quan, C. (2014). The effects of shRNA-mediated gene silencing of transcription factor SNAI1 on the biological phenotypes of breast cancer cell line MCF-7. Mol. Cell. Biochem. 388, 113–121.

43. He, Q., Zhao, L., Liu, X., Zheng, J., Liu, Y., Liu, L., Ma, J., Cai, H., Li, Z., and Xue, Y. (2019). MOV10 binding circ-DICER1 regulates the angiogenesis of glioma via miR-103a-3p/miR-382-5p mediated ZIC4 expression change. J. Exp. Clin. Cancer Res. 38, 9.

44. Jia, P., Cai, H., Liu, X., Chen, J., Ma, J., Wang, P., Liu, Y., Zheng, J., and Xue, Y. (2016). Long non-coding RNA H19 regulates glioma angiogenesis and the biological behavior of glioma-associated endothelial cells by inhibiting microRNA-29a. Cancer Lett. 381, 359–369.

45. He, Q., Zhao, L., Liu, Y., Liu, X., Zheng, J., Yu, H., Cai, H., Ma, J., Liu, L., Wang, P., et al. (2018). circ-SHKBP1 Regulates the Angiogenesis of U87 Glioma-Exposed Endothelial Cells through miR-544a/FOXP1 and miR-379/FOXP2 Pathways. Mol. Ther. Nucleic Acids 10, 331–348.

46. Liu, X., Zheng, J., Xue, Y., Yu, H., Gong, W., Wang, P., Li, Z., and Liu, Y. (2018). PIWIL3/OIP5-AS1/miR-367-3p/CEBPA feedback loop regulates the biological behavior of glioma cells. Theranostics 8, 1084–1105.

47. Cai, H., Liu, W., Xue, Y., Shang, X., Liu, J., Li, Z., Wang, P., Liu, L., Hu, Y., and Liu, Y. (2015). Roundabout 4 regulates blood-tumor barrier permeability through the modulation of ZO-1, Occludin, and Claudin-5 expression. J. Neuropathol. Exp. Neurol. 74, 25–37.

48. Cheng, J., Maier, K.C., Avsec, Ž., Rus, P., and Gagneur, J. (2017). Cis-regulatory elements explain most of the mRNA stability variation across genes in yeast. RNA 23, 1648–1659.